Subcellular localization of phosphatidylinositol 4,5-bisphosphate using the pleckstrin homology domain of phospholipase C δ_1

Stephen A. WATT, Gursant KULAR, Ian N. FLEMING, C. Peter DOWNES and John M. LUCOCQ[1]

School of Life Sciences, MSI/WTB Complex, University of Dundee, Dow Street, Dundee DD1 5EH, Scotland, U.K.

Ptd(4,5)P_2 is thought to promote and organize a wide range of cellular functions, including vesicular membrane traffic and cytoskeletal dynamics, by recruiting functional protein complexes to restricted locations in cellular membranes. However, little is known about the distribution of PtdIns(4,5)P_2 in the cell at high resolution. We have used the pleckstrin homology (PH) domain of phospholipase δ_1 (PLCδ_1), narrowly specific for PtdIns(4,5)P_2, to map the distribution of the lipid in astrocytoma and A431 cells. We applied the glutathione S-transferase-tagged PLCδ_1 PH domain (PLCδ_1PH–GST) in an on-section labelling approach which avoids transfection procedures. Here we demonstrate PtdIns(4,5)P_2 labelling in the plasma membrane, and also in intracellular membranes, including Golgi (mainly stack), endosomes and endoplasmic reticulum, as well as in electron-dense structures within the nucleus. At the plasma membrane, labelling was more concentrated over lamellipodia, but not in caveolae, which contained less than 10% of the total cell-surface labelling. A dramatic decrease in signal over labelled compartments was observed on preincubation with the cognate headgroup [Ins(1,4,5)P_3], and plasma-membrane labelling was substantially decreased after stimulation with thrombin-receptor-activating peptide (SFLLRN in the one-letter amino acid code), a treatment which markedly diminishes PtdIns(4,5)P_2 levels. Thus we have developed a highly selective method for mapping the PtdIns(4,5)P_2 distribution within cells at high resolution, and our data provide direct evidence for this lipid at key functional locations.

Key words: immunoelectron microscopy, immunogold, lipid domains, localization, phosphoinositide.

INTRODUCTION

The minor membrane phospholipid PtdIns(4,5)P_2 has a long-established role as a precursor of signalling molecules. These include InsP_3 and diacylglycerol [1], generated after hydrolysis of PtdIns(4,5)P_2 by phospholipases, and PtdIns(3,4,5)P_3 generated by the phosphorylation of PtdIns(4,5)P_2 by phosphoinositide 3-kinases downstream of membrane-bound receptors [2–4]. PtdIns(4,5)P_2 has more recently been proposed to play a more direct role as local organizer of diverse cellular activities, such as membrane trafficking [5] and cytoskeleton dynamics [6,7]. The emerging paradigm proposes that exquisite degrees of spatial and temporal control are achieved when specialized membrane domains contain high concentrations of PtdIns(4,5)P_2 [8,9]. These domains act as foci for recruitment of functional protein complexes and, depending on the process involved, may either cover large portions of an organelle membrane or alternatively very small submicron-sized patches also referred to as 'microdomains' or 'rafts' [10]. In this scheme, the spatial restriction is driven by local synthesis or clustering of the lipid, followed by recruitment of functional protein complexes by specific lipid-binding domains such as pleckstrin homology (PH) [11], **F**ab1p, **Y**OTB, **V**ac1p and **E**EA1 ('FYVE') domains [12] or Phox homology ('PX') domains [13].

While these mechanisms are attractive, there are still few direct *in situ* data to support restricted distributions for signalling lipids such as PtdIns(4,5)P_2, especially on intracellular organelles. Some evidence for restricted spatial distribution of PtdIns(4,5)P_2 at the plasma membrane comes from localization studies utilizing green fluorescent protein (GFP)–PH domain probes. These have demonstrated spatially segregated pools of PtdIns(4,5)P_2 associated with sites of phagocytosis, exocytosis [14] or agonist-stimulated ruffling activity [15,16]. In the case of phagocytosis and ruffling, PtdIns(4,5)P_2 concentration occurs in large micron-sized patches of cell membrane which recruit actin and also PtdIns(4)P 5-kinases possibly engaged in local synthesis of PtdIns(4,5)P_2 [17]. Biochemical experiments too have suggested the existence of PtdIns(4,5)P_2 domains in which a high proportion of hormone-responsive PtdIns(4,5)P_2 was found in caveolin-rich detergent-insoluble fractions [18], implying that the PtdIns(4,5)P_2 was located in caveolae. Consistent with this idea, depletion of cholesterol disrupted the association of PtdIns(4,5)P_2 with these complexes [19], although no direct evidence for large pools of PtdIns(4,5)P_2 in caveolae has been forthcoming. Finally, at the plasma membrane, there is also a strong expectation that focal accumulations of PtdIns(4,5)P_2 promote recruitment of proteins involved in the biogenesis and process of clathrin-coated-pit endocytosis (including AP180, epsin and dynamin) [20,21], but, again, the proposed domains have not been observed directly.

Within the cell, spatially restricted PtdIns(4,5)P_2 may be important in maintaining Golgi organization and facilitating protein transport. The Golgi scaffold protein spectrin contains a PtdIns(4,5)P_2-binding PH domain, and overexpression of this domain blocks transport through the Golgi [22]. Interestingly some of the lipid kinases involved in PtdIns(4,5)P_2 synthesis are recruited and activated by the small GTPase ARF (ADP ribosylation factor). ARF is a key regulator of the COPI transport vesicle formation that is restricted to specific locations on Golgi membranes [23,24]. Finally, recent data has highlighted a role for PtdIns(4,5)P_2 in transcript processing in the nucleus [25]. PtdIns(4,5)P_2 appeared to be localized to granular structures, which displayed a marked cell-cycle dependent variation in distribution.

Abbreviations used: PH, pleckstrin homology; GST, glutathione S-transferase; GFP, green fluorescent protein; PLCδ_1, phospholipase C δ_1; MVB, multivesicular bodies; EM, electron microscopy; C.E., coefficient of error; ARF, ADP ribosylation factor; SFLLRN, one-letter amino acid code for thrombin-receptor-activating peptide.

[1] To whom correspondence should be addressed (e-mail j.m.lucocq@dundee.ac.uk).

Clearly at all these sites it will be crucial to map the distribution of PtdIns(4,5)P_2 in fine detail. One of the current approaches for localization of intracellular PtdIns(4,5)P_2 uses GFP-tagged pleckstrin homology domain from the N-terminus of phospholipase C δ_1 (PLCδ_1). GFP–PH PLCδ_1 binds strongly and specifically to both PtdIns(4,5)P_2 and its soluble headgroup, Ins(1,4,5)P_3 [11]. The GFP method used in combination with confocal or deconvolution microscopy is a useful approach, but there are a number of problems associated with its use. Firstly, it has limited resolution (approx. 200 nm), even though the expected size of membrane domains could be as small as 10–50 nm, depending on the process. Secondly, GFP technology uses overexpression of PH domains within the cytosol, which may have deleterious effects on cell function either by sequestering lipid or by promoting functionally important protein–protein interactions; this is highlighted in studies showing that overexpressed GFP-tagged oxysterol-binding protein blocks trafficking in the secretory pathway [26]. For these reasons we have sought to apply PH domains as probes for quantitative mapping of lipids on ultrathin sections using electron microscopy (EM) combined with immunogold methods.

Thus far only a few ultrastructural studies have addressed the high-resolution localization of PtdIns(4,5)P_2 in cellular membranes [27]. The main reason has been lack of specific probes for EM localization and also that conventional EM may not fix and immobilize lipids that can become extracted during processing [28]. Here we use the recombinant tagged PLCδ_1PH as a probe for PtdIns(4,5)P_2 in a low-temperature on-section immunolabelling procedure to map PtdIns(4,5)P_2 distribution. Our results show that PtdIns(4,5)P_2 is present at high levels in the plasma membrane, as expected. In addition we find that PtdIns(4,5)P_2 becomes concentrated in lamellipodia, although not in caveolae. Smaller intracellular pools were detected in Golgi, endosomes and endoplasmic reticulum. In support of recent functional data [25], the method also detects substantial pools of PtdIns(4,5)P_2 in the nucleus. The present study therefore establishes low-temperature immuno-EM microscopic methods for quantitative fine structural localization of PtdIns(4,5)P_2, which will become useful for mapping other signalling lipids using suitable PH domains and other lipid-binding protein domains.

MATERIALS AND METHODS

Materials

HEK-293 and 1321N1 astrocytoma cells were obtained from the American Type Culture Collection. Cell-culture reagents were all obtained from Life Technologies.

Thrombin-receptor-activating-peptide (SFLLRN in the one-letter amino acid code) was synthesized by the MRC Protein Phosphorylation Unit of this University. Inositol phosphates were from Cell Signals (Lexington, KY, U.S.A.). Anti-[glutathione S-transferase (GST)] antibody was obtained from Chemicon International, Inc.(Temecula, CA, U.S.A.). Anti-GFP antibody was a gift from Dr Ken Sawin (Institute of Cell and Molecular Biology, University of Edinburgh, Edinburgh, Scotland, U.K.), 2C11 anti-PtdIns(4,5)P_2 antibody was a gift from Dr Giampetro Schiavo [Imperial Cancer Research Fund Laboratories (now Cancer Research U.K.), London, U.K.].

Buffers

Buffer A comprised 1% Triton X-100, 150 mM NaCl, 50 mM Tris/HCl, pH 7.4, 1 mM EGTA, 1 mM EDTA, 10 μg/ml antipain, 10 μg/ml leupeptin, 1 mM PMSF, 500 μM sodium orthovanadate, 10 mM NaF and 1 mM dithiothreitol. Buffer B comprised 150 mM NaCl, 50 mM Tris/HCl, pH 7.4, 1 mM dithiothreitol. TTBS comprised 50 mM Tris/HCl, pH 8.0, 0.1% Tween and 150 mM NaCl.

Cell culture

HEK-293 and 1321N1 astrocytoma cells were maintained in Dulbecco's modified Eagle's medium supplemented with 10% (v/v) fetal-bovine serum, 100 units/ml penicillin, 100 μg/ml streptomycin and 2 mM L-glutamine at 37 °C in a humidified atmosphere of 5% CO_2. For stimulation of 1321N1 cells with SFLLRN, the cells were grown to around 80% confluency on 10-cm-diameter plastic culture dishes. The cells were washed in PBS and SFLLRN added in fresh medium at a final concentration of 100 μM. After addition of SFLLRN, the cells were fixed at time points between 0 and 5 min by adding twice-strength fixative in 0.4 M Pipes, pH 7.2, to the medium to achieve a final concentration of 2% (v/v) glutaraldehyde (Agar Scientific, Stansted, Essex, U.K.).

Transfections and microscopical analysis

HEK-293 cells were plated out either on 15-mm-diameter coverslips in six-well tissue-culture dishes (for light microscopy) or on 10-cm-diameter plastic culture dishes (for EM) and grown to 10–20% confluency before being transfected by calcium phosphate precipitation, essentially as described previously [29]. A 10 μg portion of DNA (5 μg for 6-well plates) was added to each dish along with buffer for calcium phosphate precipitation [Hepes-buffered saline (1.5 mM $Na_2HPO_4 \cdot H_2O$/137 mM NaCl/0.55 mM Hepes, pH 7.0)/100 mM $CaCl_2$, dissolved in MilliQ-generated pure water]. The cells were left overnight at 37 °C for about 16 h before washing with warm PBS, adding fresh medium and then leaving for approx. 24 h. The cells were then washed with ice-cold PBS and then fixed. For immunofluorescence cells were fixed with 4% (w/v) paraformaldehyde/PBS, and for immunoEM cells were fixed with 8% (w/v) paraformaldehyde in 0.2 M Pipes, pH 7.2. All coverslips were mounted on slides using Hydromount mounting medium (National Diagnostics, Atlanta, GA, U.S.A.) containing 1,4-diazadicyclo[2.2.2]octane ('DABCO') and viewed on a Zeiss 410 laser scanning confocal microscope.

For immunoEM, cells were scraped from the dish using a rubber policeman and pelleted at 12000 ***g*** for 30 min (in fixative) before being infiltrated in 2.1 M sucrose overnight. Small fragments of pellets were then mounted on iron panel pins and frozen in liquid nitrogen before cutting ultrathin cryosections on a Leica EM FCS ultracut UCT microtome. Sections were picked up on droplets of 2.3 M sucrose and mounted on Pioloform (polyvinyl butyral)/carbon-coated 150-mesh hexagonal support grids and immunolabelled with affinity-purified rabbit antibodies against GFP, followed by 8 nm-particle-diameter Protein A–gold [30], essentially as described by Cheung et al. [31]. Sections were then contrasted using methylcellulose/uranyl acetate (1.8 and 0.3% respectively). Sections were viewed, and photographs taken, on a JEOL 1200EX electron microscope at 80 kV.

Preparation, expression and purification of the GST–PH domain

PCR primers were designed as described in [26] to amplify the N-terminal PH domain of PLCδ_1 (amino acids 15–180) from skeletal-muscle cDNA libraries (Clontech). The resulting PH domain contained flanking *Eco*RI and *Xba*I restriction sites to

allow directional cloning into appropriate expression vectors. The construct was verified by nucleic acid sequencing, then subcloned into a pGEX-4T vector (Pharmacia) to allow expression of GST-tagged protein in *Escherichia coli*, and into a pEGFP vector to allow expression of GFP-tagged PH domain in mammalian cells.

pGEX-4T constructs encoding the PH domain of PLCδ_1 were transformed into BL21 (DE3) pLys s *E. coli* cells and a 500 ml culture was grown in Luria broth containing 100 μg/ml ampicillin at 37 °C to an attenuance (D_{600}) of 0.6. Isopropyl β-D-thiogalactoside (0.25 mM) was added and the cells were cultured for a further 16 h at 26 °C. The cells were resuspended in 25 ml of ice-cold Buffer A, freeze–thawed once, and lysates prepared by sonication. The lysates were clarified by centrifugation (20000 ***g*** for 30 min at 4 °C) and the supernatants rocked with 1 ml of GSH–agarose beads for 1 h. Beads were collected by centrifugation (5 min at 3000 ***g***), then washed three times with Buffer A containing 0.5 M NaCl, and then a further three times with Buffer B. GST–proteins were eluted from the beads with Buffer B containing 20 mM glutathione. Eluted proteins were dialysed and snap-frozen.

Protein/lipid overlay assay

To assess the phosphoinositide-binding properties of each PH domain, a protein/lipid overlay assay was performed using GST-fusion proteins as described previously [32]. A 1 μl portion of lipid solution, dissolved in chloroform/methanol/water (1:2:0.8, by vol.), and containing various amounts of the indicated lipids (between 1 and 250 pmol), was spotted on Hybond-C extra nitrocellulose membrane and allowed to dry at room temperature for 1 h. The membrane was blocked in 2 % (w/v) fatty-acid-free BSA in TTBS for 1 h. The membrane was then incubated overnight at 4 °C with gentle stirring in the same solution containing 0.2 μg/ml of the indicated GST-fusion protein. The membranes were then washed six times over the next 30 min in TTBS, then incubated for 1 h with anti-GST monoclonal antibody (Sigma) (1:1000). Membranes were washed as described above, then incubated for 1 h with a 1:5000 dilution of anti-mouse IgG–horseradish peroxidase conjugate (Pierce). Finally, the membranes were washed 12 times over 1 h in TTBS. GST-fusion proteins bound to the membranes were then visualized by enhanced chemiluminescence (ECL®, Amersham). For competition experiments, the procedure was carried as described above, except 20 μM of the indicated inositol headgroup was added at the same step as the GST-fusion protein.

Labelling PtdIns(4,5)P_2 using PLCδ_1PH–GST in ultrathin cryosections

The principle of this approach was to prepare ultrathin thawed cryosections and incubate them with PLCδ_1PH–GST, followed by antibodies against GST and Protein A–gold. Initial studies showed that, when grid-mounted sections were exposed to room temperature at any time, there was significant staining of the grid film outside the cell profiles. This labelling could be inhibited specifically by InsP_3 headgroups and was likely due to PtdIns(4,5)P_2 release from the membranes. This effect could be completely abolished by using a modified pick up method [33] and by labelling and contrasting at ice temperature as follows. The sections were transferred to the grid within the microtome chamber (at about −100 °C) and the pick-up solution allowed to freeze on the wire pick-up loop. The droplet of pick-up solution was allowed to thaw to just above 0 °C and the grids transferred to ice-cold distilled water in porcelain dishes kept on ice, and the whole immunolabelling procedure was carried out on ice or in a cold room, making sure all solutions were pre-chilled. The grids were incubated first on 0.1 M NH_4Cl in PBS (10 min), PBS containing 0.5 % fish-skin gelatin (Sigma) for 10 min and then on droplets of PLCδ_1PH–GST (approx. 5 μg/ml) in PBS containing 0.5 % fish-skin gelatin for 20 min. Following washes in PBS, the GST was localized using anti-GST antibodies and Protein A–gold essentially as described in [31].

Quantification of immunolabelling

To assess the proportion of gold labelling found over intracellular structures, EM support grid squares containing optimally preserved and labelled pellet profiles were selected and scanned systematically at a primary magnification of 20000× (final magnification 200000×) with a random start at the corner of the EM support grid. Gold particles were assigned to compartments and the percentage over each compartment calculated. Approx. 200 gold particles were counted for each condition. To assess labelling densities over compartments, the pellet profile was scanned as described above, but in this case intersections of compartment membranes with the top edge of a clearly defined feature on the viewing screen were also counted (magnification was 20000×, but in the case of SFLLRN experiments, 40000× was used). Gold particles were related to the number of intersections over each compartment (total 150–300 intersections per condition) to give a measure of labelling density. In the case of lamellipodia, micrographs were taken at a primary magnification of 15000× and scanned on a flat-bed scanner at 1200 dpi (dots per inch) and overlaid with a 0.5 μm-square lattice grid in Adobe Photoshop 5.5. Gold and intersections with plasma membrane/lamellipodia were counted and the boundary length estimated using formulae as described by Lucocq [34]. To estimate gold labelling density over nucleoplasm and cytosol, micrographs were taken at a magnification of 12000×, scanned into Adobe Photoshop 5.5 and square lattice grids applied as described for lamellipodia above. Grid corners (points) falling over compartments of interest were counted and areas estimated from the product of the sum of these point hits and the real area of each grid lattice square (0.25 μm^2).

RESULTS

Localization of expressed GFP-tagged PLCδ_1PH

In order to determine the cellular distribution of the PtdIns(4,5)P_2-binding PH domain from PLCδ_1, we transiently expressed the PH domain fused to GFP (PLCδ_1PH–GFP) in HEK-293 cells. As described previously [35], confocal microscopy (Figure 1A) revealed fluorescence limited to the periphery of transfected cells, consistent with the large pool of PtdIns(4,5)P_2 known to exist in the plasma membrane. However, this fluorescence method did not provide evidence for smaller intracellular pools which may be present. To address this question we localized the expressed PLCδ_1PH–GFP by quantitative immunoEM on thawed cryosections using polyclonal antibodies to GFP followed by Protein A–gold (Figure 1B). We found gold labelling mainly located on the plasma membrane, but in this instance smaller amounts of PLCδ_1PH–GFP were also detected over intracellular structures. Quantification of gold labelling (Figure 2), done by systematically scanning grid cell profiles and assigning gold particles to specific cellular compartments, showed that between 60 and 70 % of gold labelling was present in the plasma membrane, with smaller proportions present over the nucleus,

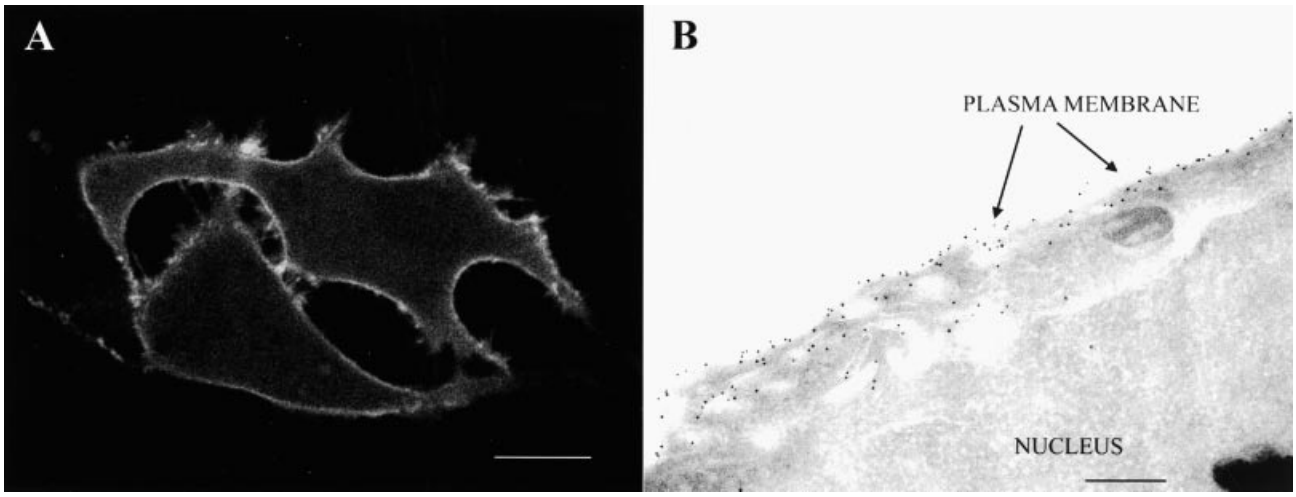

Figure 1 Localization of PLCδ_1PH–GFP by confocal and immunoEM

PLCδ_1PH-GFP was expressed in HEK-293 cells and visualized using confocal microscopy (**A**) or immunoEM (**B**) as described in the Materials and methods section. For immunoEM, ultrathin thawed cryosections were incubated with affinity-purified rabbit anti-GFP antibodies, followed by detection of bound antibodies using 8-nm-diameter Protein A–gold particles. Scale bars 10 μM in (**A**) and 200 nm in (**B**).

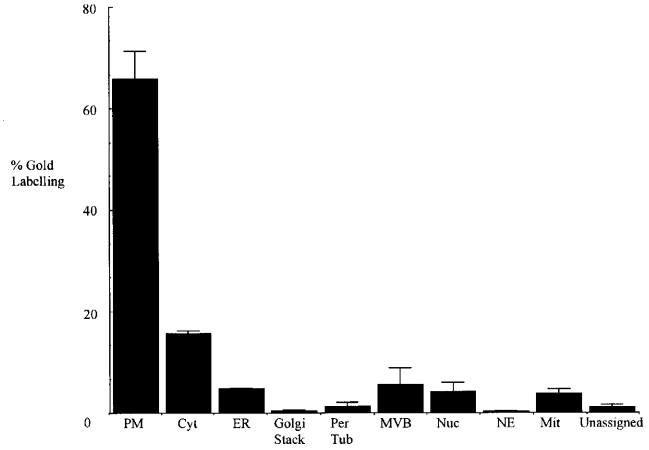

Figure 2 Quantification of PLCδ_1PH–GFP labelling over cellular compartments

PLCδ_1PH–GFP was expressed in HEK-293 cells and the cells processed for immunoEM. Randomly selected grid squares were scanned, and gold particles were assigned to specific cellular compartments as described in the Materials and methods section. Abbreviations: PM, plasma membrane; Cyt, cytosol; ER, endoplasmic reticulum; Golgi Stack, stacked Golgi cisternae; Per Tub, peripheral tubules (putative early endosomes); MVB, multivesicular bodies (limiting and internal membranes); Nuc, nucleus; NE, nuclear envelope; Mit, mitochondria; Unassigned, gold particles associated with indistinct structures. Values are the mean of three independent experiments (error bars represent S.E.M. values).

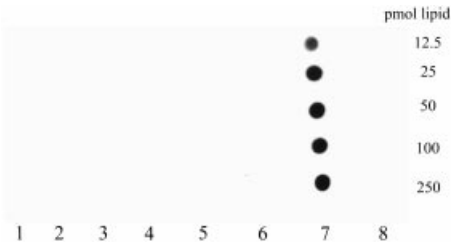

Figure 3 Demonstration of the phosphoinositide-binding specificity of PLCδ_1PH–GST

The binding specificity of PLCδ_1PH–GST was determined using a protein/lipid overlay assay. Serial dilutions of the indicated lipids were spotted on to nitrocellulose membranes that were then incubated with the purified PLCδ_1PH–GST. The membranes were washed, and bound PLCδ_1PH–GST detected using a rabbit anti-GST antibody as described in the Materials and methods section. Lanes: 1, PtdIns; 2, PtdIns3*P*; 3, PtdIns4*P*; 4, PtdIns5*P*; 5, PtdIns(3,4)P_2; 6, PtdIns(3,5)P_2; 7, PtdIns(4,5)P_2; 8, PtdIns(3,4,5)P_3.

cytosol, endoplasmic reticulum, endosomes and Golgi. These results demonstrate that, *in vivo*, PLCδ_1PH–GFP localizes to membranes of intracellular membranous organelles and to the nucleus, in addition to the plasma membrane.

Phosphoinositide localization using an on-section labelling approach

Overexpression of the GFP chimaeras within cells may have effects on the levels or distribution of endogenous lipids, and possibly disturb cellular functions dependent on phosphoinositides. In order to avoid such problems, we developed an *in situ* labelling approach that localizes the lipid present in structures displayed on ultrathin sections of untransfected cells. To this end we used PLCδ_1PH–GST as a probe for PtdIns(4,5)P_2. We first examined the specificity of this probe using protein/lipid overlay assay, and this analysis showed that PLCδ_1PH–GST was highly specific for PtdIns(4,5)P_2, and displayed no significant binding to any of seven related phosphoinositides (Figure 3). We next applied the PLCδ_1PH–GST to ultrathin sections of 1321N1 astrocytoma and A431 cells and detected the probe using an antibody to GST followed by electron-dense Protein A–gold.

The probe was applied to thawed ultrathin frozen cryosections and also sections of freeze-substituted cells embedded in the methacrylate/acrylate Lowicryl resin (HM23). Both methods produced labelling over membrane structures, but in the present study we concentrated on thawed cryosections on which the signals were higher and the display of intracellular membrane structures was more clearly defined. Lipids may not

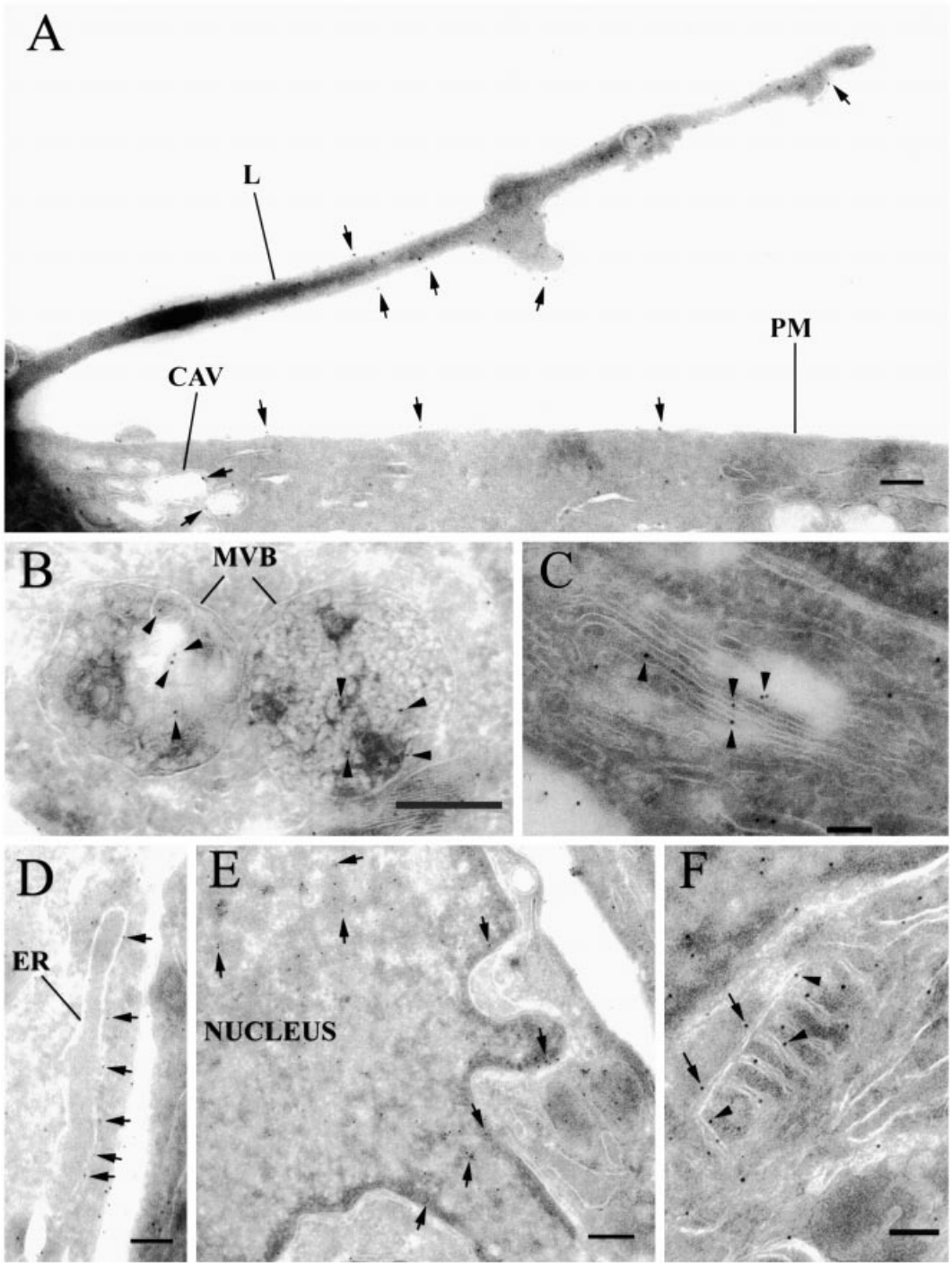

Figure 4 PLCδ_1PH–GST immunogold labelling on ultrathin thawed cryosections of 1321N1 astrocytoma cells

In (**A**) PLCδ_1PH–GST labelling (arrows) is visualised on the plasma membrane (PM), caveolae (CAV) and lamellipodia (L). In (**B**) PLCδ_1PH–GST labelling (arrowheads) is located on the internal vesicles of multivesicular bodies (MVB) and in (**C**) over cisternae of the Golgi stack (arrowheads). Arrows in (**D**) and (**E**) indicate PLCδ_1PH–GST labelling of the endoplasmic-reticulum membrane (ER) and electron-dense nuclear structures respectively. In (**F**) labelling is shown over a mitochondrion profile, both on the outer membrane (arrows) and on inner membrane and cristae (arrowheads). Scale bars: (**A**, **C**, **D** and **F**), 100 nm; (**B**), 250 nm ; (**E**), 200 nm.

be fully immobilized after aldehyde fixation, and so an important methodological modification was to limit the movement of lipids in the sections by carrying out the labelling procedure close to 0 °C (see the Materials and methods section). In 1321N1 astrocytoma cells, (Figure 4), gold labelling for PLCδ_1PH–GST was present over a variety of organelles, including plasma membrane, Golgi, endoplasmic reticulum, multivesicular bodies, mitochondria, nucleus and also caveolae which were identified by labelling with anti-(caveolin-1) antibodies (results not shown). Similar qualitative results were obtained in A431 cells (results not

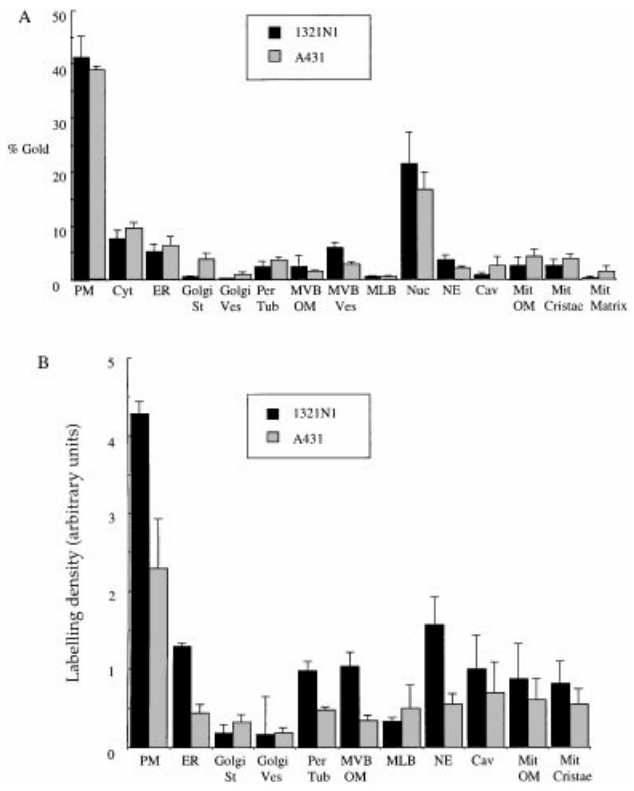

Figure 5 Quantification of PLCδ_1PH–GST immunogold labelling over cellular compartments

The proportion of PLCδ_1PH–GST labelling over individual compartments by on-section labelling is shown in (**A**) as percentages of the total gold particles counted, estimated by scanning cell profiles and assigning gold particles to compartments (see the Materials and methods section). The results are the means for three independent experiments, with approx. 200 gold particles counted for each experiment. Abbreviations, PM, plasma membrane; Cyt, cytosol; ER, endoplasmic reticulum; Golgi St, Golgi stack; Golgi Ves, Golgi vesicles; Per Tub, peripheral tubules (putative early endosomes); MVB OM, multivesicular-body outer limiting membrane; MVB Ves, multivesicular-body inner vesicles; MLB, multilamellar body; Nuc, nucleus; NE, nuclear envelope; Cav, caveolae; Mit OM, mitochondrial outer membrane; Mit Cristae, mitochondrial cristae; Mit Matrix, mitochondrial matrix. The labelling densities over membrane compartments are shown in (**B**), in which the number of gold particles were related to the number of intersections a scanning line makes with membranes from each compartment, as described in the Materials and methods section. The results are means for three independent experiments, in which 150–300 intersections were counted per experiment. Data for inner vesicles of MVBs are not reported because these structures are too small for reliable estimates to be obtained. Error bars in (**A**) and (**B**) are the S.E.M.s.

shown). Quantification revealed similar distributions of labelling in 1321N1 astrocytoma and A431 cells, with the highest proportion of labelling over the plasma membrane (Figure 5A; $\approx 40\,\%$ of total gold labelling). Nuclear labelling was also substantial, (17–21 % of total) and was particularly concentrated on electron-dense patches of heterochromatin. Lower proportions of labelling were also detected on other membranous structures, including endoplasmic reticulum, nuclear envelope, Golgi, caveolae-like structures, peripheral endosome-like tubules, multivesicular bodies (82 % labelling over internal vesicles and 18 % over the limiting membrane, $n = 95$ gold particles) and mitochondria (51 % on outer membrane and 49 % on inner membrane, $n = 39$ gold particles). A count of gold particles over the Golgi apparatus of 1321N1 astrocytoma cells showed 77 % of gold particles were found on the cisternae of the Golgi stack, with 23 % found on the membranes of Golgi-associated tubulovesicular profiles ($n = 87$ gold particles).

Under homogeneous labelling conditions the proportion of gold labelling reports on the relative amounts of available PtdIns(4,5)P_2 in organellar membranes. However, the local concentration of the lipid is likely to be a key factor in generating PtdIns(4,5)P_2-related effects within cells. We therefore also estimated the densities of labelling over membrane profiles in various cell compartments. The plasma membrane had the highest density of labelling, with significant densities observed over endoplasmic reticulum, nuclear envelope, endosomes, caveolae and mitochondrial membranes (Figure 5B), suggesting significant concentrations of PtdIns(4,5)P_2 in these organelles. Interestingly, in 1321N1 astrocytomas, the concentration of labelling over both the Golgi and the limiting membrane of multilamellar endosomes was lower than over other organelles, although this effect was not so marked in A431 cells.

Subdomains labelling for PtdIns(4,5)P_2 at the plasma membrane

Caveolae are specialized invaginated domains of the plasma membrane enriched in cholesterol and implicated in transmembrane signalling [36]. Previous studies suggested that substantial proportions of PtdIns(4,5)P_2 are concentrated in these structures, and so we carried out a quantitative analysis of PLCδ_1PH–GST labelling in caveolae. This showed that caveolae of 1321N1 astrocytoma cells (identified by immunogold labelling for caveolin 1; results not shown) held only 3.6 % of the total labelling, and 8 % of labelling over the plasma membrane and caveolae combined (corresponding data for A431 cells were 2.5 and 5.9 % respectively). The labelling density over caveolae was roughly similar to that over putative endosomes (peripheral tubular structures and multivesicular-body limiting membranes), but was markedly lower than over the plasma membrane, arguing against the notion of high concentrations of PtdIns(4,5)P_2 in these structures (Figure 5B).

Previous studies using PLCδ_1PH–GFP have indicated that PtdIns(4,5)P_2 is concentrated in specialized regions of the plasma membrane, such as membrane ruffles/lamellipodia. Since 1321N1 astrocytoma cells appear to undergo constitutive formation of lamellipodia, we estimated the immunogold labelling density over plasma membrane and lamellipodia-like profiles using the PLCδ_1PH–GST probe. We found that lamellipodia-like cell extensions had a labelling density of 6.7 gold particles/μm [coefficent of error (C.E.) 13.5 %; n = seven micrographs], whereas the rest of the plasma membrane had a density of 3.34 gold particles/μm (C.E. 11.9 %; n = seven micrographs). Lamellipodia-like profiles contained 39 % of the total plasma-membrane labelling (see Figure 4).

Inhibition of lipid binding with inositol headgroups

To test the specificity of the labelling with the PLCδ_1PH–GST fusion protein, we carried out competition experiments by preincubating PLCδ_1PH–GST with the soluble inositol lipid headgroup of PtdIns(4,5)P_2, Ins(1,4,5)P_3. Previous studies indicated that Ins(1,4,5)P_3 binds around 8-fold more strongly to PLCδ_1 than does PtdIns(4,5)P_2 (K_d 0.21 μM versus 1.7 μM; [11]) and in protein/lipid overlay assay this head group completely prevented binding (Figure 6, upper panel). Preincubation of PLCδ_1PH–GST with Ins(1,4,5)P_3 resulted in drastic reductions in gold labelling over all labelled intracellular membranes and, for 1321N1 astrocytoma cells, quantification of this effect is displayed in Figure 6 (lower panel) (results for A431 cells not shown). This

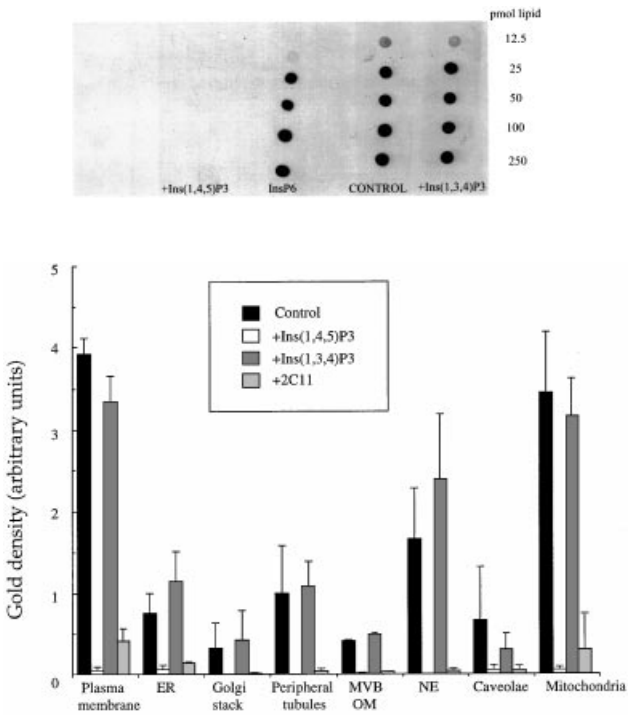

Figure 6 Inhibition of PLCδ_1PH–GST binding by inositol phosphate headgroup competition

Upper panel: the effect of inositol phosphate headgroups on PLCδ_1PH–GST binding to PtdIns(4,5)P_2 was assessed by performing a protein/lipid overlay assay. Serial dilutions of PtdIns(4,5)P_2 were spotted on to nitrocellulose membrane, which was incubated with PLCδ_1PH–GST (control) or PLCδ_1PH–GST pre-mixed with various inositol headgroups. Membranes were washed and bound PLCδ_1PH–GST detected using an anti-GST antibody. Lower panel: ultrathin cryosections were prepared as described in the Materials and methods section and labelled using PLCδ_1PH–GST, followed by rabbit anti-GST antibodies and Protein A–gold. In control incubations PLCδ_1PH–GST was preincubated with either 1 mM Ins(1,4,5)P_3 or Ins(1,3,4)P_3 (a non-cognate headgroup) prior to the labelling sequence. As a further test of specificity the 2C11 anti-PtdIns(4,5)P_2 antibody was preincubated on ultrathin cryosections before incubating with PLCδ_1PH–GST. Labelling densities were then estimated by relating gold particles and intersections over specific compartments. Results for each condition are the means for three independent experiments done on 1321N1 astrocytoma cells. Error bars represent S.E.M.s.

Table 1 Decrease in endogenous PtdIns(4,5)P_2 levels in the plasma membrane using SFLLRN

1321N1 cells were stimulated for various times (0–300 s) with SFLLRN in order to decrease PtdIns(4,5)P_2 levels. These cells were then processed for ultrathin cryosectioning and incubated with PLCδ_1PH–GST by the on-section labelling procedure. Labelling densities over the plasma membrane were then calculated by relating the number of gold particles to the number of intersections over the plasma membrane for each condition (see the Materials and methods section). Three grid squares were scanned for each condition and approx. 50 intersections counted. Values are means ± S.E.M. for three experiments. Gold labelling density is expressed as particles/intersection (a) or as a percentage of the untreated value (b).

(a)

Time after SFLLRN stimulation (s)	Density (gold particles per intersection)
Untreated	8.9 ± 1.56
10	7.1 ± 0.84
30	5.85 ± 0.44
300	10.12 ± 1.6

(b)

Time after SFLLRN stimulation (s)	Density (% of untreated value)
Untreated	100 ± 17.5
10	79.8 ± 9.4
30	65.7 ± 4.9
300	113 ± 17.9

headgroup also reduced labelling over cytosolic and nuclear compartments. For cytosol, labelling was 4.91 (S.E.M. 0.64, $n = 10$) gold/μm^2 with PLCδ_1PH–GST alone and 1.03 (S.E.M. 0.2, $n = 10$) gold/μm^2 with PLCδ_1PH–GST/Ins(1,4,5)P_3. For nucleus, labelling was 18.132 (S.E.M. 2.08, $n = 10$) gold/μm^2 with PLCδ_1PH–GST alone and 0.2 (S.E.M. 0.2, $n = 10$) gold/μm^2 with PLCδ_1PH-GST/Ins(1,4,5)P_3. To rule out a general inhibitory effect of negatively charged headgroups, we also used Ins(1,3,4)P_3, the headgroup of PtdIns(3,4)P_2. This headgroup did not inhibit binding of PLCδ_1PH–GST to cellular membranes (Figure 6, lower panel), cytosol or nucleus (results not shown) or to PtdIns(4,5)P_2 in the protein/lipid overlay assay (Figure 6, upper panel). Lack of inhibition on protein/lipid overlay and on ultrathin sections was also observed for the headgroup Ins(1,4)P_2 (results not shown) and for InsP_6, which has been reported to bind weakly to PLCδ_1 [37] (Figure 6, upper panel; results for on-section labelling not shown).

An additional test of the specificity of the probe was to preincubate sections with the anti-PtdIns(4,5)P_2 antibody 2C11 in order to block potential binding sites for the PH domain [25]. By protein/lipid overlay, this antibody has specificity for both PtdIns4P and PtdIns(4,5)P_2 (results not shown) and labels plasma membrane and intracellular structures by EM (results not shown). Preincubation of ultrathin sections with this antibody again resulted in a substantial reduction of labelling on all labelled membrane-bound compartments (Figure 6, lower panel) as well as cytosol and nucleus. Together the data presented here therefore provide strong evidence that the labelling on EM sections is related to PtdIns(4,5)P_2.

Modulation of endogenous PtdIns(4,5)P_2 levels

In order to assess further the specificity of the PH-domain probe we performed an experiment to modulate the endogenous levels of PtdIns(4,5)P_2 and correlate quantities of labelling with PLC δ_1PH–GST. 1321N1 astrocytoma cells were stimulated for various times (between 0 and 5 min) with SFLLRN before fixation. Stimulation of the thrombin receptor with SFLLRN activates phospholipase C enzymes, which hydrolyse PtdIns(4,5)P_2. Previous work has demonstrated that SFLLRN evokes a transient decrease in PtdIns(4,5)P_2 levels over a 30 s period before returning to resting levels over the subsequent 5 min [38]. Stimulated cells were cryosectioned, labelled with PLCδ_1PH–GST as described above, and then labelling densities over the plasma membrane estimated. As can be seen in Table 1, stimulation with SFLLRN resulted in a decrease in the density of labelling, which was at its lowest after 30 s of stimulation and gradually returned to pre-stimulation levels after 5 min – essentially the same pattern as seen in previous experiments [38]. The maximum fall in labelling density was approx. 35%. These results provide additional support for the view that the on-section labelling detects PtdIns(4,5)P_2 and further demonstrate the suitability of this PH-domain probe as a tool for phosphoinositide localization.

DISCUSSION

We have developed an *in situ* high-resolution approach for the localization of PtdIns(4,5)P_2 using lipid-binding PH domains. Following aldehyde fixation, ultrathin sections are affinity decorated with the epitope-tagged PH domain, followed by localizing antibodies and electron-dense Protein A–gold. Such an on-section labelling approach has a number of distinct advantages. First, sectioning is an efficient way of presenting the membranes of intracellular compartments and their component lipids directly to the labelling system without permeabilization of the cells. Secondly, it avoids transfection with fluorescent tagged PH domains, a strategy which can alter cell function by sequestering lipid or by promoting/interfering with protein–protein interactions, as exemplified in studies on oxysterol-binding protein [26] and PLCδ_1 [39]. Thirdly, on-section labelling is not dependent on transfection to introduce lipid probes, and the lipid distribution can now be studied in any cell or tissue that can be adequately fixed and sectioned. One potential problem with the method is that many lipids, including phosphoinositides, may not be well immobilized after aldehyde fixation [28]. However this problem appears to be resolved by keeping the sections near to ice temperature throughout the handling and labelling procedures – a strategy that reduces diffusion of the lipid to a minimum, as evidenced by the lack of spreading of specific labelling out from the plasma membrane.

Our results are consistent with major pools of PtdIns(4,5)P_2 both at the plasma membrane and also in intracellular organelles. But how specific is the labelling? The PH domain of PLCδ_1 has high affinity and selectivity for PtdIns(4,5)P_2 ($K_d = 1.7\ \mu$M; [40]), suggesting that it is highly specific for PtdIns(4,5)P_2 in membranes exposed on our sections. To confirm further the specificity we preincubated the GST-tagged PH domain with the cognate headgroup possessing phosphorylations at the 4- and 5-positions of the inositol ring [Ins (1,4,5)P_3]. Ins(1,4,5)P_3 abolished interaction in protein/lipid overlays and was extremely potent in reducing subsequent labelling on-sections. InsP_3 with phosphorylations at the 3- and 4-positions [Ins (1,3,4)P_3] did not inhibit labelling. Significantly, an antibody raised against PtdIns(4,5)P_2, which in lipid/protein overlays binds to both PtdIns(4,5)P_2 and PtdIns4*P*, was also able to reduce interactions of the GST-labelled PH domain with the sections.

Further evidence for the validity of the PtdIns(4,5)P_2 labelling approach comes from SFLLRN stimulation experiments. Previous work has shown that such treatment of astrocytoma cells causes a transient decrease in PtdIns(4,5)P_2 labelling at the plasma membrane, which returns to pre-stimulation levels after about 5 min [38]. As reported here, the PLCδ_1PH–GST labelling densities showed a similar pattern at the plasma membrane after treatment with SFLLRN, suggesting that PLCδ_1PH–GST labelling may be useful as a quantitative estimator of local PtdIns (4,5)P_2 concentrations. In this regard it is worth emphasizing this method is likely to detect only PtdIns(4,5)P_2 available to the labelling system and not necessarily PtdIns(4,5)P_2 already bound to proteins. Thus, depending on the proportion of PtdIns(4,5)P_2 bound to proteins, there is a potential for the labelling approach used here to under-report on amounts of PtdIns(4,5)P_2. Nevertheless, taken together our results indicate the method successfully labels those intracellular pools of PtdIns(4,5)P_2 accessible to the labelling system on the surface of ultrathin cryosections. Interestingly, the experiments with SFLLRN may suggest an explanation for the observed cytosolic labelling using the PLCδ1PH–GST probe. The cytosolic signal could be due to tangentially sectioned membrane structures not visible in the section, or to small amounts of lipid relocated during or after sectioning. Alternatively it could represent Ins*P*3 generated by hydrolysis of plasma-membrane-located PtdIns(4,5)P_2 [41]. This possibility is consistent with a small, but reproducible, increase in labelling we have observed over the cytosol (but not nucleus) during thrombin-receptor stimulation (J. M. Lucocq and S. Watt, unpublished work). However, this needs further investigation, because InsP_3 is soluble and unlikely to be cross-linked by aldehydes and would need to be complexed to cytosolic proteins or other components to be retained in ultrathin sections.

The plasma membrane is a primary site of PtdIns(4,5)P_2 synthesis, but the precise distribution of the lipid within the membrane is currently unclear. We therefore analysed the labelling distribution and density in plasma-membrane domains that could be distinguished in sections, including caveolae [42] and lamellipodia. Previous data have suggested that caveolae, defined as detergent-insoluble lipid domains enriched in caveolin, might contain a substantial proportion of cellular PtdIns(4,5)P_2 and that this PtdIns(4,5)P_2 is hormone-responsive [18]. Further studies also indicated that PtdIns(4,5)P_2 was associated with caveolin and that the association could be disrupted using cholesterol-sequestering agents such as cyclodextrin [19]. Our PtdIns(4,5)P_2 localization study detected less than 10 % of the total cell-surface labelling in caveolae and found no evidence for concentration of labelling within these structures in either A431 or astrocytoma cells. It is therefore unlikely that the majority of PtdIns(4,5)P_2 resides in caveolar cholesterol-rich domains and points more towards the existence of non-caveolar domains containing PtdIns(4,5)P_2. It will now be important to map the distribution of PtdIns(4,5)P_2 in the plane of the membrane using freeze–fracture techniques and attempt to identify such domains. We also found increased concentrations of PtdIns(4,5)P_2 in lamellipodia of 1321N1 astrocytoma cells, and this is consistent with previous work indicating a role for the lipid in agonist-stimulated ruffling and resulting phagocytosis [15–17]. The quantitative read-out provided by this lipid labelling method should provide novel correlative insights into the location of PtdIns (4,5)P_2 and its effectors on ruffling structures.

We also found PLCδ_1PH-GST labelling on the rough endoplasmic reticulum, Golgi structures and endosomes, providing direct *in situ* evidence for pools of PtdIns(4,5)P_2 in the secretory and endocytic pathways. Our endoplasmic-reticulum data are consistent with studies showing phosphatidylinositol synthase activity and PtdIns(4,5)P_2 synthesis [43,44] in microsomal fractions. More specifically, phosphatidylinositol 4-kinase α, as well as a novel phosphatidylinositol-5-phosphate 4-kinase (phosphatidylinositol-phosphate kinase IIγ), has been identified on endoplasmic-reticulum membranes [45,46], and a yeast PtdIns(4,5)P_2 5-phosphatase Inp54 located on the endoplasmic reticulum exerts negative control of secretion [47]. Studies are in progress to analyse the role of PtdIns(4,5)P_2 in the early secretory pathway in mammalian cells. In the Golgi we found 25 % of PtdIns(4,5)P_2 labelling was located over tubulovesicular structures, with a major proportion (75 %) over the cisternal stack. The tubulovesicular structures most likely contain a population of COPI-coated transport vesicles whose formation may depend on PtdIns(4,5)P_2. PtdIns(4,5)P_2 is is an activator of the small GTPase ARF, which drives recruitment of COPI coats and also promotes further rounds of PtdIns(4,5)P_2 via recruitment and activation of PtdIns(4,5)P_2-synthesizing enzymes [23,24]. We are currently searching for small microdomain platforms involved in vesicle biogenesis within the Golgi membrane reticulum [8]. Interestingly, the high proportion of labelling on the Golgi stack may indicate a role for PtdIns(4,5)P_2 in maintenance of Golgi structure, perhaps by regulating scaffold proteins such as

spectrin, which is known to possess a PtdIns(4,5)P_2-binding PH domain [48].

Here we also demonstrate a significant proportion of labelling for PtdIns(4,5)P_2 over the nucleus, mitochondria and, to a lesser extent, over the cytosolic compartment (discussed above). The nuclear label corresponds to about 20 % of the total PtdIns(4,5)P_2 labelling in the cell and is in line with previous studies demonstrating that both phosphoinositides and their biosynthetic machinery are found in the nucleus [25,49,50]. A number of roles have been assigned to nuclear phosphoinositides, including chromatin remodelling, pre-mRNA splicing or as precursor of signalling intermediates such as diacylglycerol or InsP_3. We have not analysed the distribution of PtdIns(4,5)P_2 labelling in detail, but the labelling of electron-dense structures in the nucleoplasm is in agreement with a recent report using the 2C11 antibody [25]. The exquisite specificity of the PLCδ_1-PH domain should make it a valuable tool for analysing the role of Ptd*P*-like molecules in nuclear function. Finally, the mitochondrial labelling is intriguing, because reports of PtdIns(4,5)P_2-like lipids or PtdIns(4,5)P_2-synthesizing enzymes in mitochondrial membranes are at present very limited indeed [51,52].

In summary, we have developed a method for mapping PtdIns(4,5)P_2 in eukaryotic cells using the PH domain of PLCδ_1, and demonstrated that PtdIns(4,5)P_2 is distributed both on the plasma membrane and in localized intracellular pools. The further development of such tools [53] in affinity localization of phosphoinsitides at high resolution, combined with methods for studying membranes in three dimensions, should provide a much deeper understanding of how local concentrations of these lipids drive and organize key intracellular processes such as membrane traffic and cytoskeletal dynamics.

J.M.L. was supported by a Research Leave Fellowship from the Wellcome Trust (059767/Z/99/Z) and by Tenovus Scotland. S.A.W. is a CASE (Co-operative Awards in Science and Engineering) Ph.D. student supported by the Biotechnology and Biological Sciences Research Council (BBSRC) and the Nissei Sangyo Co Ltd. Technical help was provided by Calum Thomson and John James. We also thank Wiebke Moebius for helpful discussions on lipid labelling protocols. We are grateful to Giampetro Schiavo [Imperial Cancer Research Laboratories (now Cancer Research U.K.), London, U.K.] and Ken Sawin (Institute of Cell and Molecular Biology, Edinburgh, Scotland, U.K.) for generously providing antibodies and to Alan Prescott for help with confocal microscopy. C.P.D. was supported by grants 053684/BS/JM (post-doctoral fellowship to G.K.) and G9900995 from the Wellcome Trust and the Medical Research Council (MRC) respectively.

REFERENCES

1 Berridge, M. J. and Irvine, R. F. (1989) Inositol phosphates and cell signalling. Nature (London) **341**, 197–205
2 Cross, D. A., Alessi, D. R., Cohen, P., Andjelkovich, M. and Hemmings, B. A. (1995) Inhibition of glycogen synthase kinase-3 by insulin mediated by protein kinase B. Nature (London) **378**, 785–789
3 Kohn, A. D., Kovacina, K. S. and Roth, R. (1995) Insulin stimulates the kinase activity of RAC-PK, a pleckstrin homology domain containing Ser/Thr kinase. EMBO **14**, 4288–4295
4 Stephens, L. R., Hughes, K. T. and Irvine, R. F. (1991) Pathway of phosphatidylinositol(3,4,5)-trisphosphate synthesis inactivated neutrophils. Nature (London) **351**, 33–39
5 De Camilli, P., Emr, S. D., McPherson, P. S. and Novick, P. (1996) Phosphoinositides as regulators in membrane traffic. Science **271**, 1533–1539
6 Janmey, P. A. (1994) Phosphoinositides and calcium as regulators of cellular actin assembly and disassembly. Annu. Rev. Physiol. **56**, 169–191
7 Fukami, K., Endo, T., Imamura, M. and Takenawa, T. (1994) α-Actinin and vinculin are PIP_2-binding proteins involved in signaling by tyrosine kinase. J. Cell Biol. **269**, 1518–1522
8 Simonsen, A., Wurmser, A. E., Emr, S. D. and Stenmark, H. (2001) The role of phosphoinositides in membrane transport. Curr. Opin. Cell Biol. **13**, 485–492
9 Martin, T. F (2001) PI(4,5)P(2) regulation of surface membrane traffic. Curr. Opin. Cell Biol. **13**, 493–499
10 Simons, K. and Toomre, D. (2000) Lipid rafts and signal transduction. Nat. Rev. Mol. Cell Biol. **1**, 31–39
11 Lemmon, M. A. and Ferguson, K. M. (2000) Signal-dependent membrane targeting by pleckstrin homology (PH) domains. Biochem J. **350**, 1–18
12 Gillooly, D. J., Simonsen, A. and Stenmark, H. (2001) Cellular functions of phosphatidylinositol 3-phosphate and FYVE domain proteins. Biochem. J. **355**, 249–258
13 Simonsen, A. and Stenmark, H. (2001) PX domains: attracted by phosphoinositides. Nat. Cell Biol. **3**, E179–E182
14 Bajno, L., Peng, X. R., Schreiber, A. D., Moore, H. P., Trimble, W. S. and Grinstein, S. (2000) Focal exocytosis of VAMP3-containing vesicles at sites of phagosome formation. J. Cell Biol. **149**, 697–706
15 Honda, A., Nogami, M., Yokozeki, T., Yamazaki, M., Nakamura, H., Watanabe, H., Kawamoto, K., Nakayama, K., Morris, A. J., Frohman, M. A. and Kanaho, Y. (1999) Phosphatidylinositol 4-phosphate 5-kinase α is a downstream effector of the small G protein ARF6 in membrane ruffle formation. Cell **99**, 521–532
16 Tall, E. G., Spector, I., Pentyala, S. N., Bitter, I. and Rebecchi, M. J. (2000) Dynamics of phosphatidylinositol 4,5-bisphosphate in actin-rich structures. Curr. Biol. **10**, 743–746
17 Botelho, R. J., Teruel, M., Dierckman, R., Anderson, R., Wells, A., York, J. D., Meyer, T. and Grinstein, S. (2000) Localized biphasic changes in phosphatidylinositol-4,5-bisphosphate at sites of phagocytosis. J. Cell Biol. **151**, 1353–1368
18 Pike, L. J. and Casey, L. (1996) Localization and turnover of phosphatidylinositol 4,5-bisphosphate in caveolin-enriched membrane domains. J. Biol. Chem. **271**, 26453–26456
19 Pike, L. J. and Miller, J. M. (1998) Cholesterol depletion delocalizes phosphatidylinositol bisphosphate and inhibits hormone-stimulated phosphatidylinositol turnover. J. Biol. Chem. **273**, 22298–22304
20 Cremona, O. and De Camilli, P. (2001) Phosphoinositides in membrane traffic at the synapse. J. Cell Sci. **114**, 1041–1052
21 Itoh, T., Koshiba, S., Kigawa, T., Kikuchi, A., Yokoyama, S. and Takenawa, T. (2001) Role of the ENTH domain in phosphatidylinositol-4,5-bisphosphate binding and endocytosis. Science **291**, 993–994
22 Martin, T. F. (2001) PI(4,5)P_2 regulation of surface membrane traffic. Curr. Opin. Cell Biol. **13**, 493–499
23 Godi, A., Pertile, P., Meyers, R., Marra, P., Di Tullio, G., Iurisci, C., Luini, A., Corda, D. and De Matteis, M. A. (1999) ARF mediates recruitment of PtdIns-4-OH kinase-β and stimulates synthesis of PtdIns(4,5)P_2 on the Golgi complex. Nat. Cell Biol. **1**, 280–287
24 Jones, D. H., Morris, J. B., Morgan, C. P., Kondo, H., Irvine, R. F. and Cockcroft, S. (2000) Type I phosphatidylinositol 4-phosphate 5-kinase directly interacts with ADP-ribosylation factor 1 and is responsible for phosphatidylinositol 4,5-bisphosphate synthesis in the Golgi compartment. J. Biol. Chem. **275**, 13962–13966
25 Osborne, S. L., Thomas, C. L., Gschmeissner, S. and Schiavo, G. (2001) Nuclear PtdIns(4,5)P_2 assembles in a mitotically regulated particle involved in pre-mRNA splicing. J. Cell Sci. **114**, 2501–2511
26 Levine, T. P. and Munro, S. (1998) The pleckstrin homology domain of oxysterol-binding protein recognises a determinant specific to Golgi membranes. Curr. Biol. **8**, 729–739
27 Voorhout, W. F., van Genderen, I. L., Yoshioka, T., Fukami, K., Geuze, H. J. and van Meer, G. (1992) Subcellular localisation of glycolipids as revealed by immuno-electron microscopy. Trends Glycosci. Glycotechnol. **4**, 533–546
28 Griffiths, G. (1993) Fine structure preservation. In Fine Structure Immunocytochemistry (Griffiths, G., Burke, B. and Lucocq, J., eds.), pp. 26–80, Springer-Verlag, Berlin
29 Ponnambalam, S., Rabouille, C., Luzio, J. P., Nilsson, T. and Warren, G. (1994) The TGN38 glycoprotein contains two non-overlapping signals that mediate localization to the *trans*-Golgi network. J. Cell Biol. **125**, 253–268
30 Lucocq, J. M. (1993) Particulate markers for immunoelectron microscopy. In Fine Structure Immunocytochemistry (Griffiths, G., Burke, B. and Lucocq, J., eds.), pp. 279–302, Springer-Verlag, Berlin
31 Cheung, P. C. F., Trinkle-Mulcahy, L., Cohen, P. and Lucocq, J. M. (2001) Characterization of a novel phosphatidylinositol 3-phosphate-binding protein containing two FYVE fingers in tandem that is targeted to the Golgi. Biochem. J. **355**, 113–121
32 Fleming, I. N., Gray, A. and Downes, C. P. (2000) Regulation of the Rac1-specific exchange factor Tiam1 involves both phosphoinositide 3-kinase-dependent and -independent components. Biochem. J. **351**, 173–182
33 Liou, W., Geuze, H. J. and Slot, J. W. (1996) Improving structural integrity of cryosections for immunogold labelling. Histochem. Cell. Biol. **106**, 41–58
34 Lucocq, J. M. (1994) Quantitation of gold labelling and antigens in immunolabelled ultrathin sections. J. Anat. **184**, 1–13
35 Varnai, P. and Balla, T. (1998) Visualization of phosphoinositides that bind pleckstrin homology domains: calcium- and agonist-induced dynamic changes and relationship to *myo*-[^{3}H]inositol-labeled phosphoinositide pools. J. Cell Biol. **143**, 501–510
36 Marx, J. (2001) Caveolae: A once-elusive structure gets some respect. Science **294**, 1862–1865

37 Lemmon, M. A., Ferguson, K. M., O'Brien, R., Sigler, P. B. and Schlessinger, J. (1995) Specific and high-affinity binding of inositol phosphates to an isolated pleckstrin homology domain. Proc. Natl. Acad. Sci. U.S.A. **92**, 10472–10476
38 Batty, I. H. and Downes, C. P. (1996) Thrombin receptors modulate insulin-stimulated phosphatidylinositol 3,4,5-trisphosphate accumulation in 1321N11 astrocytoma cells. Biochem. J. **317**, 347–351
39 Raucher, D., Stauffer, T., Chen, W., Shen, K., Guo, S., York, J. D., Sheetz, M. P. and Meyer, T. (2001) Phosphatidylinositol 4,5-bisphosphate functions as a second messenger that regulates cytoskeleton-plasma membrane adhesion. Cell **100**, 221–228
40 Lemmon, M. A., Ferguson, K. M. and Schlessinger, J. (1996) PH domains: diverse sequences with a common fold recruit signaling molecules to the cell surface. Cell **85**, 621–624
41 Nash, M. S., Young, K. W., Willars, G. B., Challiss, R. A. and Nahorski, S. R. (2001) Single-cell imaging of graded Ins(1,4,5)P_3 production following G-protein-coupled-receptor activation. Biochem. J. **356**, 137–142
42 Schlegel, A. and Lisanti, M. P. (2001) Caveolae and their coat proteins, the caveolins: from electron microscopic novelty to biological launching pad. J. Cell Physiol. **186**, 329–337
43 Helms, J. B., de Vries, K. J. and Wirtz, K. W. (1991) Synthesis of phosphatidylinositol 4,5-bisphosphate in the endoplasmic reticulum of Chinese hamster ovary cells. J. Biol. Chem. **266**, 21368–21374
44 Lundberg, G. A. and Jergil, B. (1988) Generation of phosphatidylinositol 4,5-bisphosphate proceeds through an intracellular route in rat hepatocytes. FEBS Lett. **240**, 171–176
45 Wong, K., Meyers, R. and Cantley, L. C. (1997) Subcellular locations of phosphatidylinositol 4-kinase isoforms. J. Biol. Chem. **272**, 13236–13241
46 Itoh, T., Ijuin, T. and Takenawa, T. (1998) A novel phosphatidylinositol-5-phosphate 4-kinase (phosphatidylinositol-phosphate kinase IIgamma) is phosphorylated in the endoplasmic reticulum in response to mitogenic signals. J. Biol. Chem. **273**, 20292–20299
47 Wiradjaja, F., Ooms, L. M., Whisstock, J. C., McColl, B., Helfenbaum, L., Sambrook, J. F., Gething, M. J. and Mitchell, C. A. (2001) The yeast inositol polyphosphate 5-phosphatase Inp54p localizes to the endoplasmic reticulum via a C-terminal hydrophobic anchoring tail: regulation of secretion from the endoplasmic reticulum. J. Biol. Chem. **276**, 7643–7653
48 De Matteis, M. A. and Morrow, J. S. (2000) Spectrin tethers and mesh in the biosynthetic pathway. J. Cell Sci. **113**, 2331–2343
49 Mazzotti, G., Zini, N., Rizzi, E., Rizzoli, R., Galanzi, A., Ognibene, A., Santi, S., Matteucci, A., Martelli, A. M. and Maraldi, N. M. (1995) Immunocytochemical detection of phosphatidylinositol 4,5-bisphosphate localization sites within the nucleus. J. Histochem. Cytochem. **43**, 181–191
50 Maraldi, N. M., Zini, N., Santi, S. and Manzoli, F. A. (1999) Topology of inositol lipid signal transduction in the nucleus. J. Cell Physiol. **181**, 203–217
51 Bothmer, J., Markerink, M. and Jolles, J. (1992) Evidence for a new inositol phospholipid in rat brain mitochondria. Biochem. Biophys. Res. Commun. **187**, 1077–1082
52 Balla, A., Vereb, G., Gulkan, H., Gehrmann, T., Gergely, P., Heilmeyer, Jr., L. M. and Antal, M. (2000) Immunohistochemical localisation of two phosphatidylinositol 4-kinase isoforms, PI4K230 and PI4K92, in the central nervous system of rats. Exp. Brain Res. **134**, 279–288
53 Dowler, S., Currie, R. A., Campbell, D. G., Deak, M., Kular, G., Downes, C. P. and Alessi, D. R. (2000) Identification of pleckstrin-homology-domain-containing proteins with novel phosphoinositide-binding specificities. Biochem. J. **351**, 19–31

Received 3 October 2001/24 January 2002; accepted 28 February 2002